



Evidence for three-dimensional Fermi-surface topology of the layered electron-doped iron superconductor $\text{Ba}(\text{Fe}_{1-x}\text{Co}_x)_2\text{As}_2$

P. Vilmercati,^{1,2} A. Fedorov,³ I. Vobornik,⁴ U. Manju,⁴ G. Panaccione,⁴ A. Goldoni,⁵ A. S. Sefat,⁶ M. A. McGuire,⁶ B. C. Sales,⁶ R. Jin,^{1,6} D. Mandrus,⁶ D. J. Singh,⁶ and N. Mannella^{1,*}

¹*Department of Physics and Astronomy, The University of Tennessee, Knoxville, Tennessee 37996, USA*

²*Dipartimento di Fisica, Università degli Studi di Trieste, I-34127 Trieste, Italy*

³*Advanced Light Source, Lawrence Berkeley National Laboratory, Berkeley, California 94720, USA*

⁴*TASC National Laboratory, INFN-CNR, SS 14, km 163.5, I-34012 Trieste, Italy*

⁵*Sincrotrone Trieste S.C.p.A., Area Science Park, SS 14, km 163.5, I-34012 Trieste, Italy*

⁶*Materials Science and Technology Division, Oak Ridge National Laboratory, Oak Ridge, Tennessee 37831, USA*

(Received 4 February 2009; revised manuscript received 20 April 2009; published 4 June 2009)

The electronic structure of electron-doped iron-arsenide superconductors $\text{Ba}(\text{Fe}_{1-x}\text{Co}_x)_2\text{As}_2$ has been measured with angle-resolved photoemission spectroscopy. The data reveal a marked photon energy dependence of points in momentum space where the bands cross the Fermi energy, a distinctive and direct signature of three dimensionality in the Fermi-surface topology. By providing a unique example of high-temperature superconductivity hosted in layered compounds with three-dimensional electronic structure, these findings suggest that the iron arsenides are unique materials, quite different from the cuprates high-temperature superconductors.

DOI: [10.1103/PhysRevB.79.220503](https://doi.org/10.1103/PhysRevB.79.220503)

PACS number(s): 74.25.Jb, 74.70.-b, 79.60.-i

The recent discovery of high-temperature superconductivity in Fe-based superconductors (FeSC) has provided the opportunity of studying high-temperature superconductivity and its relation to magnetism in a wide range of magnetic element-based materials.¹ Cuprate high-temperature superconductors (HTSC) and FeSC materials are the only two families of compounds with superconducting critical temperature (T_c) known to exceed 55 K. It is therefore important to determine whether and to what extent these two classes of materials are similar. Much like in cuprates, superconductivity in FeSC emerges in close proximity to a long-range-ordered antiferromagnetic ground state, indicating that the interplay between superconductivity and spin-density-wave instability is likely important in FeSC.²⁻⁵ On the other hand, spectroscopic evidence has shown that the electronic structure of both the superconducting and normal state is quite different from that of cuprates.⁶⁻⁸ Despite their layered structure, $(\text{Ba},\text{K})\text{Fe}_2\text{As}_2$ materials have recently been reported to exhibit superconducting properties that are in fact quite isotropic, a behavior drastically different compared to that of other layered superconductors.⁹ It has been proposed that the nearly isotropic critical field of $(\text{Ba},\text{K})\text{Fe}_2\text{As}_2$ might be linked to its distinctive three-dimensional electronic structure and Fermi-surface (FS) topology, indicating that the reduced dimensionality is not a prerequisite for high-temperature superconductivity, contrary to what has been suggested for cuprate HTSC. A direct determination of the dimensionality of the electronic structure and FS topology in FeSC materials is thus timely and important, as it is expected to provide firm grounds of comparison for establishing commonalities and differences with the cuprate HTSC.

In this Rapid Communication, we address this issue by reporting the results of angle-resolved photoemission spectroscopy (ARPES) measurements of the electronic structure in the normal state of BaFe_2As_2 and $\text{BaFe}_{1.8}\text{Co}_{0.2}\text{As}_2$ single crystals. The data reveal a marked three-dimensional charac-

ter of the electronic band structure and FS topology for both the parent and doped compounds.

The $\text{Ba}(\text{Fe}_{1-x}\text{Co}_x)_2\text{As}_2$ materials crystallize in high-quality single crystals with the tetragonal ThCr_2Si_2 structure type (space group $I4/mmm$) and have a maximum $T_c=22$ K for $x=0.1$ nominal doping.¹⁰ Electron probe microanalysis carried out with a JEOL JSM-840 scanning electron microprobe on several crystals indicated that 8.0(5)% of the Fe is replaced by Co in BaFe_2As_2 . This composition will be represented as the nominal $\text{BaFe}_{1.8}\text{Co}_{0.2}\text{As}_2$ or 8% Co doping. Co doping of the BaFe_2As_2 system is advantageous since electronic carriers are added directly in the FeAs planes and Co is easier to handle than alkali metals. In remarkable contrast to cuprates HTSC, the BaFe_2As_2 system appears to tolerate considerable disorder in the FeAs planes. High-quality single crystals were grown out of FeAs flux according to modalities described elsewhere.¹⁰ The ARPES measurements were carried out on beamline 10.0.1 and beamline 12.0.1 at the Advance Light Source, and the low-energy branch of the APE-INFN beamline in Elettra Synchrotron (Trieste, Italy). Several samples from different batches have been measured at 30 K after being cleaved *in situ* in a pressure better than 3×10^{-11} Torr. The total instrumental energy resolution was 12–25 meV, while the angular resolution was set to either $\pm 0.5^\circ$ or $\pm 0.1^\circ$, which correspond to ≈ 0.05 and $\approx 0.01 \text{ \AA}^{-1}$, respectively.

The basic features of the electronic structure of the BaFe_2As_2 materials have been exposed by several ARPES investigations.^{6,11-17} The electronic structure consists of disconnected FS, a holelike pocket at the zone center (Γ), and an electronlike pocket at the zone corner (M), with the electronic bands exhibiting some renormalization effects. A direct comparison of spectra collected along the ΓX direction (i.e., $[100]$) in the parent BaFe_2As_2 and doped $\text{BaFe}_{1.8}\text{Co}_{0.2}\text{As}_2$ ($T_c=22$ K) compounds is shown in Fig. 1. Since these spectra have been collected in identical experimental conditions (same photon energy, in-plane photon po-

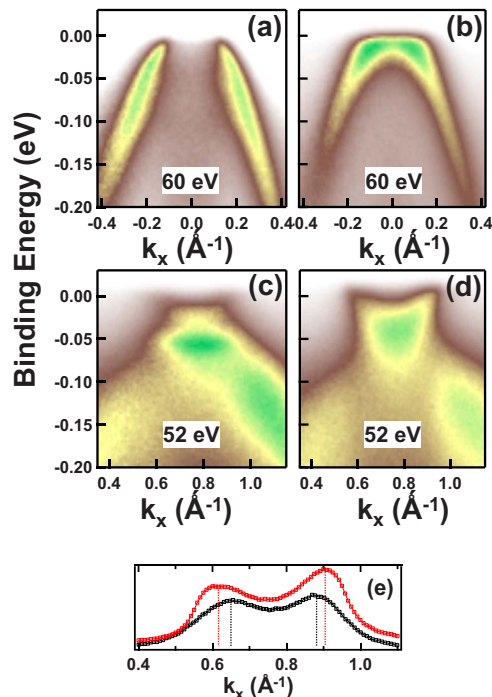


FIG. 1. (Color online) Image plots of data collected with in-plane photon polarization along the ΓX direction (i.e., $[100]$) at the Γ point in the (a) parent BaFe_2As_2 and (b) doped $\text{BaFe}_{1.8}\text{Co}_{0.2}\text{As}_2$ compounds, and at the M point for the (c) parent and (d) doped compounds, respectively. The numbers in the panels denote the photon energy used. Panel (e) shows the MDC curves at zero binding energy for the parent (black line, bottom curve) and doped (red line, top curve) compounds corresponding to the image plots in (c) and (d), respectively. Upon Co substitution, the hole pocket at Γ becomes smaller, while the electron pocket at M becomes larger, indicating that Co substitution induces an upward shift of the chemical potential, as expected for electron doping.

larization), the differences in the spectral features reflect intrinsic differences between the parent and doped compounds caused by doping. Upon Co substitution, the hole pocket at Γ becomes smaller, while the electron pocket at M becomes larger (Fig. 1). These changes are indicative of an upward shift of the chemical potential, as expected for electron doping. Similar observations occur both when using different photon energies and when spectra are collected along the ΓM direction, thus, indicating that Co substitution is indeed effective in doping the FeAs plane with electrons. Our result confirms the predictions of density-functional calculations, namely, that the Co-doped materials behave like a coherent alloy with the main effect induced by Co doping being an upward shift of the chemical potential.¹⁰ This “rigid-band” behavior contrasts what would be expected in a strongly correlated system, thus, providing another distinction between FeSC and cuprates.

ARPES is a premiere tool for measuring energy dispersion and symmetry of bulk bands.¹⁸ For electron bands dispersing along the direction perpendicular to the surface plane (the c axis), the allowed direct transitions will shift in energy and consequently in momentum perpendicular to the sample plane (k_z) when the photon energy is changed.¹⁸ Signatures

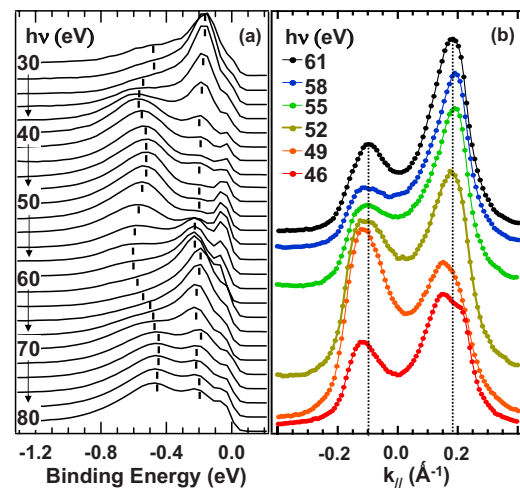


FIG. 2. (Color online) (a) $\text{BaFe}_{1.8}\text{Co}_{0.2}\text{As}_2$ valence-band spectra collected in normal emission with different photon energies. The spectra have been collected in the angular mode with the analyzer slit along the ΓM direction. The photon polarization was mixed, with both in-plane and out-of-plane components. The spectra have been integrated in a window of $\pm 1^\circ$ around the Γ point. The dispersion of the structure at ≈ 600 meV is indicative of a three-dimensional character of the band structure. (b) MDC curves at zero binding energy for $\text{BaFe}_{1.8}\text{Co}_{0.2}\text{As}_2$ collected at the M point (electron pocket) with different photon energies (top, $h\nu=61$ eV; bottom, $h\nu=46$ eV) along the GX $[100]$ direction and in-plane polarizations. The origin of the horizontal axis has been set to the k_x position of the M point ($\approx 0.79 \text{ \AA}^{-1}$).

of three-dimensional dispersion are thus typically revealed in ARPES experiments by changes in the valence-band peaks position when the spectra are collected in normal emission while changing the photon energy, as shown in Fig. 2(a). Besides the enhancement of the structure close to the Fermi level (E_F) resulting from the $\text{Fe } 3p \rightarrow \text{Fe } 3d$ resonance at $h\nu \approx 56$ eV, the spectra show dispersion of a structure with binding energy (BE) of ≈ 600 meV, a distinct signature of the three-dimensional character of this band. Also visible is another structure at 200 meV BE with weaker dispersion. The modulation of these structures exhibits a periodicity as a function of photon energy which, when translated into the k_z quantum number using a free-electron final-state approximation with an inner potential of 15 eV,¹⁸ corresponds to $\approx 1 \text{ \AA}^{-1}$, a value remarkably close to the expected periodicity along $k_z \approx 4\pi/c = 0.968 \text{ \AA}^{-1}$, with $c = 12.98 \text{ \AA}$.¹⁰

To address the possible three-dimensional character of the FS, we have carried out a systematic photon energy dependence of the states close to E_F both at the Γ point and at the M point. The data have been analyzed with momentum distribution curves (MDC), which identify as Fermi wave vectors the maximum positions of the momentum distribution of spectral weight at E_F . The MDC analysis of the spectra collected in $\text{BaFe}_{1.8}\text{Co}_{0.2}\text{As}_2$ at the M point [Fig. 2(b)] shows little changes in the Fermi crossing point, i.e., zero binding energy, for different photon energies, indicating that the electron pockets are cylinderlike with a low degree of warp, as predicted by local-density approximation (LDA) calculations.¹⁰

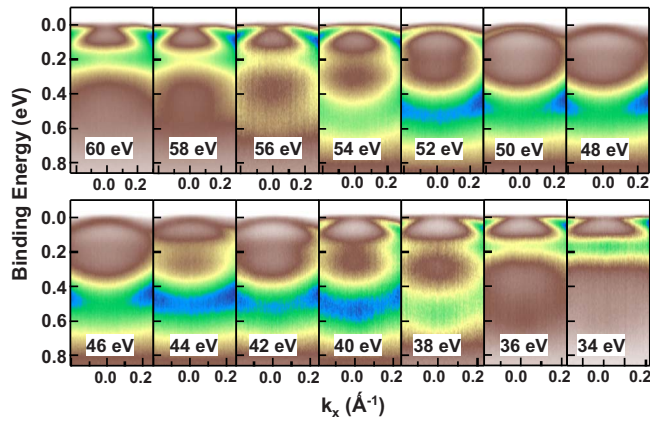


FIG. 3. (Color online) Photon energy dependence of spectra collected in $\text{BaFe}_{1.8}\text{Co}_{0.2}\text{As}_2$ at the Γ point along the ΓX direction. The numbers in the insets denote the photon energy used. The photon polarization was mixed, with both in-plane and out-of-plane components. The photon energy dependence of the Fermi crossing points at zero binding energy is evidence of the three-dimensional character of the FS topology.

Figure 3 shows spectra collected in $\text{BaFe}_{1.8}\text{Co}_{0.2}\text{As}_2$ at the Γ point along the ΓM direction $[100]$ for different photon energies and high-momentum resolution ($\approx 0.01 \text{ \AA}^{-1}$). The most noteworthy characteristic of these data is the marked dependence of the Fermi crossing points on the photon energy, which reveals a strong dispersion along the k_z direction in momentum space. Particularly interesting is also the observation of a band located $\approx 200 \text{ meV}$ below E_F . This band is predicted by LDA calculations when atom positions are obtained by relaxing the internal coordinates of the As vertical position using LDA total-energy minimization but not

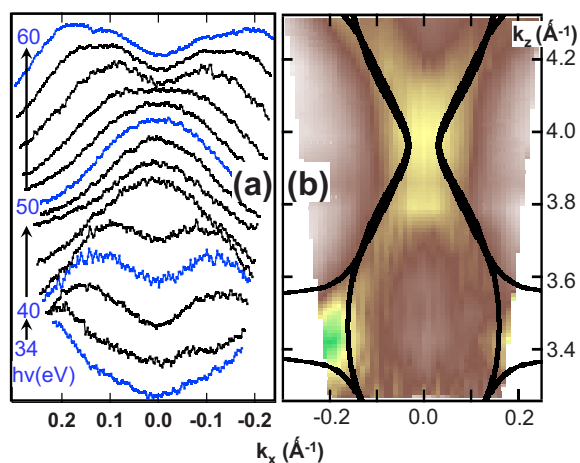


FIG. 4. (Color online) Analysis of the spectra shown in Fig. 3. (a) MDC curves at E_F and (b) intensity at E_F plotted in color scale as a function of the in-plane momentum k_x and vertical momentum k_z . The plot illustrates the three-dimensional character of the Fermi-surface topology by showing how the FS around the Γ point consists of a cylinder with small cross-sectional area that flares out in proximity of the Z point. The Γ and Z points correspond to $\approx 3.88 \text{ \AA}^{-1}$ and 3.39 \AA^{-1} on the vertical k_z scale. The continuous black line in (b) denotes the k_z dispersion calculated for $\text{BaFe}_{1.8}\text{Co}_{0.2}\text{As}_2$ with LDA in the virtual-crystal approximation.

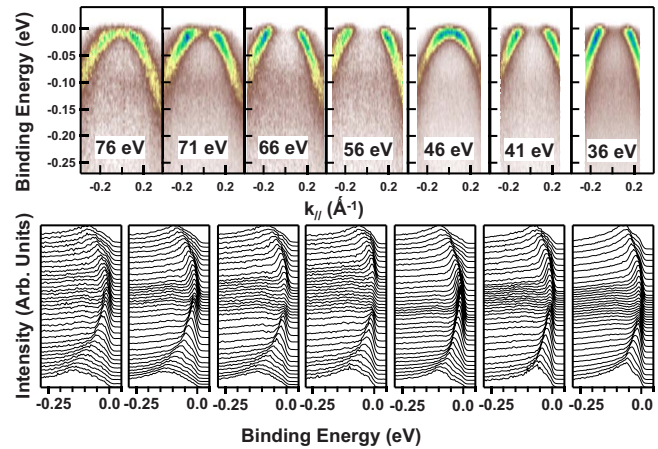


FIG. 5. (Color online) Photon energy dependence of spectra collected in the parent compound BaFe_2As_2 at the Γ point along the ΓX direction. The panels in the top and bottom rows denote the image plot and the corresponding energy distribution curves. The numbers in the insets denote the photon energy used. The photon polarization was in plane. The photon energy dependence of the Fermi crossing points at zero binding energy is evidence of the three-dimensional character of the FS topology.

when atom positions are taken from structural refinement data.¹⁹ Changes in As atom positions on the order of 0.1 \AA may occur as a result of a surface relaxation, a possibility which warrants further investigations.

In the case of well-known two-dimensional systems such as the layered manganites, layered cuprates, and organic superconductors, the FS are very two dimensional, with a cross-sectional area that varies little along the interlayer direction or— analogously— with Fermi crossing points which are insensitive to the use of different photon energies.^{20,21} This occurrence does not seem to be the case in $\text{BaFe}_{1.8}\text{Co}_{0.2}\text{As}_2$. To better illustrate this point, Fig. 4(a) shows the MDC analysis of the spectra shown in Fig. 3. The MDC curves make it apparent how the Fermi crossing points change markedly along the ΓX direction when the photon energy is changed. These data show that there is dispersion along the k_z direction, indicating a three-dimensional character of the FS topology in the FeSC compounds. LDA calculations have predicted that in $\text{Ba}(\text{Fe}_{1-x}\text{Co}_x)_2\text{As}_2$ compounds, the FS around the Γ point consists of a cylinder with small cross-sectional area that flares out in proximity of the Z point.¹⁰ Figure 4(b) shows the distribution of spectral weight at E_F in color scale as a function of the in-plane momentum along ΓX (k_x) with the out-of-plane momentum k_z displayed on the vertical axis. This plot represents a cross-sectional view of the FS profile and illustrates how considerable the dispersion along the k_z direction in momentum space is, manifested as a strong variation in the cross-sectional cut along k_x as k_z is changed, fully consistent with the LDA predictions as shown in the same figure. The three-dimensional character of the FS topology in $\text{BaFe}_{1.8}\text{Co}_{0.2}\text{As}_2$ provides a rationale for the unusual nearly isotropic critical field of $(\text{Ba},\text{K})\text{Fe}_2\text{As}_2$.⁹ Our results are also consistent with ARPES data collected with photon energies of 50 and 80 eV in Ref. 17, in which similar Fermi crossing points were

found at these two energies. This is in agreement with our data and analysis since photon energies of 50 and 80 eV correspond to similar values of k_z .²²

We have carried out similar experiments using different light polarizations. We observed that with in-plane photon polarization, it was impossible to detect the band at 200 meV, most likely a result due to matrix elements effects, which have been shown to be quite strong in the FeSC materials.¹² More importantly, the strong k_z dispersion effects shown in Fig. 3 remain observable, independent of the polarization of the incoming light. We also found that the three dimensionality of the FS topology is also a characteristic of the parent compound. Figure 5 shows data collected in BaFe₂As₂ at the Γ point, along the ΓM direction, at different photon energies, with in-plane photon polarization. The marked dependence on the photon energy of the Fermi crossing points is substantial, as much as that of the doped compound shown in Fig. 3.

The FeSC shows an intimate connection between magnetism and superconductivity. Experiments show that the undoped spin-density-wave ground state of the parent compound is metallic, as the normal states of the superconducting phases. This is in contrast to cuprates, whose undoped ground state is a Mott insulator. In cuprates, the connections between the undoped Mott insulators and the superconducting phases occur only at high energy, i.e., in the

Hubbard bands. Our results further underscore the connection in FeSC between the magnetic and superconducting phases by showing that they have a similar degree of three dimensionality.

In conclusion, it appears that FeSC are quite unique high-temperature superconductors, with an itinerant Fe d -band character, high density of states at E_F , and capable of hosting high-temperature superconductivity without the signatures of strong local Mott-Hubbard-type correlations that characterize cuprate HTSC. Furthermore, the present results show by the example of Ba(Fe_{1-x}Co_x)₂As₂ compounds that the FeSC materials have a three-dimensional FS topology, thus, indicating that reduced dimensionality is not a necessary condition for high-temperature superconductivity. These results assist in establishing a unique character of the FeSC materials, which should be considered a different type of high-temperature superconductors, quite unlike the cuprates.

The work at the ALS and Elettra is supported by the NSF under Grant No. DMR-0804902. The work at Oak Ridge is sponsored by the Division of Materials Science and Engineering, Office of Basic Energy Sciences. Oak Ridge National Laboratory is managed by UT-Battelle, LLC, for the U.S. Department of Energy under Contract No. DE-AC05-00OR22725.

*Corresponding author; nmannel@utk.edu

- ¹Y. Kamihara, T. Watanabe, M. Hirano, and H. Hosono, *J. Am. Chem. Soc.* **130**, 3296 (2008).
- ²C. de la Cruz, Q. Huang, J. W. Lynn, J. Li, W. Ratcliff II, J. L. Zarestky, H. A. Mook, G. F. Chen, J. L. Luo, N. L. Wang, and P. Dai, *Nature (London)* **453**, 899 (2008).
- ³H. Takahashi, K. Igawa, K. Arii, Y. Kamihara, M. Hirano, and H. Hosono, *Nature (London)* **453**, 376 (2008).
- ⁴F. Hunte, J. Jaroszynski, A. Gurevich, D. C. Larbalestier, R. Jin, A. S. Sefat, M. A. McGuire, B. C. Sales, D. K. Christen, and D. Mandrus, *Nature (London)* **453**, 903 (2008).
- ⁵G. F. Chen, Z. Li, D. Wu, G. Li, W. Z. Hu, J. Dong, P. Zheng, J. L. Luo, and N. L. Wang, *Phys. Rev. Lett.* **100**, 247002 (2008).
- ⁶D. H. Lu, M. Yi, S.-K. Mo, A. S. Erickson, J. Analytis, J.-H. Chu, D. J. Singh, Z. Hussain, T. H. Geballe, I. R. Fisher, and Z.-X. Shen, *Nature (London)* **455**, 81 (2008).
- ⁷F. Bondino, E. Magnano, M. Malvestuto, F. Parmigiani, M. A. McGuire, A. S. Sefat, B. C. Sales, R. Jin, D. Mandrus, E. W. Plummer, D. J. Singh, and N. Mannella, *Phys. Rev. Lett.* **101**, 267001 (2008).
- ⁸W. Malaeb, T. Yoshida, T. Kataoka, A. Fujimori, M. Kubota, K. Ono, H. Usui, K. Kuroki, R. Arita, H. Aoki, Y. Kamihara, M. Hirano, and H. Hosono, *J. Phys. Soc. Jpn.* **77**, 093714 (2008).
- ⁹H. Q. Yuan, J. Singleton, F. F. Balakirev, S. A. Baily, G. F. Chen, J. L. Luo, and N. L. Wang, *Nature (London)* **457**, 565 (2009).
- ¹⁰A. S. Sefat, R. Jin, M. A. McGuire, B. C. Sales, D. J. Singh, and D. Mandrus, *Phys. Rev. Lett.* **101**, 117004 (2008).
- ¹¹C. Liu, G. D. Samolyuk, Y. Lee, N. Ni, T. Kondo, A. F. Santander-Syro, S. L. Bud'ko, J. L. McChesney, E. Rotenberg, T. Valla, A. V. Fedorov, P. C. Canfield, B. N. Harmon, and A. Kaminski, *Phys. Rev. Lett.* **101**, 177005 (2008).
- ¹²D. Hsieh *et al.*, arXiv:0812.2289 (unpublished).
- ¹³H. Ding, P. Richard, K. Nakayama, K. Sugawara, T. Arakane, Y. Sekiba, A. Takayama, S. Souma, T. Sato, T. Takahashi, Z. Wang, X. Dai, Z. Fang, G. F. Chen, J. L. Luo, and N. L. Wang, *EPL* **83**, 47001 (2008).
- ¹⁴Y. Sekiba, T. Sato, K. Nakayama, K. Terashima, P. Richard, J. H. Bowen, H. Ding, Y.-M. Xu, L. J. Li, G. H. Cao, Z.-A. Xu, and T. Takahashi, *New J. Phys.* **11**, 025020 (2009).
- ¹⁵H. Liu, W. Zhang, L. Zhao, X. Jia, J. Meng, G. Liu, X. Dong, G. F. Chen, J. L. Luo, N. L. Wang, W. Lu, G. Wang, Y. Zhou, Y. Zhu, X. Wang, Z. Xu, C. Chen, and X. J. Zhou, *Phys. Rev. B* **78**, 184514 (2008).
- ¹⁶L. X. Yang, Y. Zhang, H. W. Ou, J. F. Zhao, D. W. Shen, B. Zhou, J. Wei, F. Chen, M. Xu, C. He, Y. Chen, Z. D. Wang, X. F. Wang, T. Wu, G. Wu, X. H. Chen, M. Arita, K. Shimada, M. Taniguchi, Z. Y. Lu, T. Xiang, and D. L. Feng, *Phys. Rev. Lett.* **102**, 107002 (2009).
- ¹⁷V. B. Zabolotnyy, D. S. Inosov, D. V. Evtushinsky, A. Koitzsch, A. A. Kordyuk, G. L. Sun, J. T. Park, D. Haug, V. Hinkov, A. V. Boris, C. T. Lin, M. Knupfer, A. N. Yaresko, B. Büchner, A. Varykhalov, R. Follath, and S. V. Borisenko, *Nature (London)* **457**, 569 (2009).
- ¹⁸E. W. Plummer and W. Eberhardt, *Adv. Chem. Phys.* **49**, 533 (1982).
- ¹⁹D. J. Singh, *Phys. Rev. B* **78**, 094511 (2008).
- ²⁰N. Mannella, W. L. Yang, X. J. Zhou, H. Zheng, J. F. Mitchell, J. Zaanen, T. P. Devereaux, N. Nagaosa, Z. Hussain, and Z.-X. Shen, *Nature (London)* **438**, 474 (2005).
- ²¹A. Damascelli, Z. X. Shen, and Z. Hussain, *Rev. Mod. Phys.* **75**, 473 (2003).
- ²²Photon energies of 50 and 80 eV correspond to k_z values of 3.99 and 4.88 \AA^{-1} , respectively, whose difference is close to the expected periodicity along $k_z \approx 4\pi/c = 0.968 \text{\AA}^{-1}$.